

Leveraging FPGAs for Homomorphic Matrix-Vector Multiplication in Oblivious Message Retrieval

Grant Bosworth*, Keewoo Lee†, and Sunwoong Kim*

*Rochester Institute of Technology, Rochester, NY, USA, †Ethereum Foundation

Email: {grb1300, sskeme}@rit.edu, keewoo.lee@ethereum.org

Abstract—While end-to-end encryption protects the content of messages, it does not secure metadata, which exposes sender and receiver information through traffic analysis. A plausible approach to protecting this metadata is to have senders post encrypted messages on a public bulletin board and receivers scan it for relevant messages. Oblivious message retrieval (OMR) leverages homomorphic encryption (HE) to improve user experience in this solution by delegating the scan to a resource-rich server while preserving privacy. A key process in OMR is the homomorphic detection of pertinent messages for the receiver from the bulletin board. It relies on a specialized matrix-vector multiplication algorithm, which involves extensive multiplications between ciphertext vectors and plaintext matrices, as well as homomorphic rotations. The computationally intensive nature of this process limits the practicality of OMR. To address this challenge, this paper proposes a hardware architecture to accelerate the matrix-vector multiplication algorithm. The building homomorphic operators in this algorithm are implemented using high-level synthesis, with design parameters for different parallelism levels. These operators are then deployed on a field-programmable gate array platform using an efficient design space exploration strategy to accelerate homomorphic matrix-vector multiplication. Compared to a software implementation, the proposed hardware accelerator achieves a $13.86\times$ speedup.

Index Terms—Design space exploration, field-programmable gate array, high-level synthesis, homomorphic encryption, oblivious message retrieval

I. INTRODUCTION

End-to-end encryption (E2EE) ensures only the sender and receiver can access a message, blocking even the service provider. However, E2EE does not effectively protect metadata, which can reveal *who communicated with whom* [1]. Metadata often enables detailed tracking of online activity, sometimes making access to message content unnecessary. A key aspect of metadata protection is receiver privacy, aiming to conceal the receiver's identity.

A plausible approach to achieving receiver privacy is to have senders post encrypted messages on a public bulletin board, allowing receivers to scan it for messages intended for them. However, this approach imposes a significant burden on receivers. To improve usability, several works have proposed delegating this costly linear scan to a server in a privacy-preserving way. Yet, these solutions either provide only a weak form of privacy [2] or rely on strong environmental assumptions, such as the availability of trusted execution environments or multiple communicating-but-non-colluding servers [3], [4].

To achieve full receiver privacy under minimal assumptions, oblivious message retrieval (OMR) was introduced by Liu and

Tromer [1], by incorporating homomorphic encryption (HE), which is a cryptographic technique that allows computations on encrypted data directly [5]. HE enables offloading the task of detecting payloads pertinent to the receiver, among those from multiple senders, from the receiver to a resource-rich third-party server. Since the introduction of the original OMR, several variants have been proposed, particularly focused on improving the efficiency of server-side operations [6], [7].

Despite its potential in various applications, such as privacy-preserving cryptocurrencies, OMR faces several practical challenges. One major issue is the slow processing speed introduced by the use of an HE scheme. To address this, we propose a field-programmable gate array (FPGA)-based accelerator for homomorphic matrix-vector multiplication, which is a key performance bottleneck in OMR. Our accelerator achieves a performance improvement of $13.86\times$ over a CPU implementation. To the best of the authors' knowledge, this is the first work on custom hardware accelerators for OMR.

II. BACKGROUND

A. BFV Homomorphic Encryption Scheme

The Brakerski–Fan–Vercauteren (BFV) scheme is one of the most widely used HE schemes, supporting integer arithmetic modulo a prime number [8], [9]. It consists of the following core stages: key generation, encoding, encryption, evaluation, decryption, and decoding. Key generation creates secret, public, and evaluation keys, based on HE parameters. Encoding takes multiple integer messages and packs them into a vector, which is then transformed into a plaintext polynomial $\text{pt} \in \mathcal{R}_t = \mathbb{Z}_t[X]/(X^n + 1)$, where t is the plaintext modulus and n is the ring dimension. Encryption uses the public key and the plaintext polynomial to generate a ciphertext $\text{ct} \in \mathcal{R}_Q \times \mathcal{R}_Q$ (i.e., two ciphertext polynomials), where $\mathcal{R}_Q = \mathbb{Z}_Q[X]/(X^n + 1)$ and Q is the ciphertext modulus. Since Q is often hundreds or thousands of bits long, large-number arithmetic is required, which is computationally inefficient in standard computing environments. To address this, the residue number system (RNS) is applied to the BFV scheme [10]. In RNS-based BFV, each ciphertext polynomial is decomposed into several smaller polynomials (known as limbs), each modulo a smaller prime q_i , such that $Q = \prod_i q_i$. These smaller polynomials can be processed independently, while still producing the same result as using the original Q .

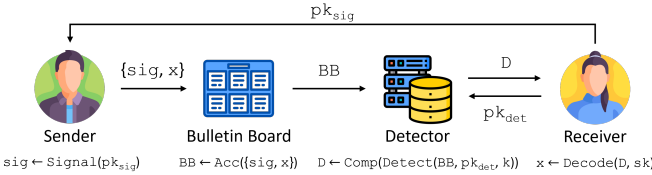


Fig. 1. Overall flow of SophOMR based on a PS technique.

Evaluation uses homomorphic operations to carry out a specific privacy-preserving application. The following are the BFV homomorphic operations, which are used in this work:

- **Ciphertext-ciphertext addition** (CCadd) performs element-wise addition of the corresponding polynomials in two ciphertexts. Given ciphertexts $ct_1 = (ct_1^{(1)}, ct_1^{(2)})$ and $ct_2 = (ct_2^{(1)}, ct_2^{(2)})$, $CCadd(ct_1, ct_2)$ is $((ct_1^{(1)} + ct_2^{(1)}) \bmod q, (ct_1^{(2)} + ct_2^{(2)}) \bmod q) = ct_3$.
- **Plaintext-ciphertext multiplication** (PCmul) multiplies a plaintext polynomial by a ciphertext, producing a new ciphertext. Given a ciphertext $ct = (ct^{(1)}, ct^{(2)})$ and a plaintext pt , $PCmul(pt, ct)$ is defined as $((ct^{(1)} \cdot pt) \bmod q, (ct^{(2)} \cdot pt) \bmod q) = ct'$.
- **Rotation operation** (Rot) shifts the slots of an encrypted vector. Let ct be a ciphertext encrypting a vector of integers $\mathbf{v} = \{v_0, v_1, \dots, v_{u-1}\}$. $Rot_a(ct)$ denotes a rotation of the ciphertext by a slots, resulting in a new ciphertext that encrypts the rotated vector $\{v_a, v_{a+1}, \dots, v_{a-1}\}$. Rot consists of two main steps: *ApplyGalois* and *KeySwitch*. *ApplyGalois* applies a Galois automorphism to the ciphertext, which rearranges its coefficients. *KeySwitch* uses rotation keys (also known as Galois keys), a type of evaluation keys, to transform the resulting ciphertext back into a form that can be decrypted using the original secret key. Compared to CCadd and PCmul, Rot is computationally more expensive. This is mainly due to the *KeySwitch* step, which involves modular multiplications with large rotation keys and number theoretic transform (NTT). For more details, refer to [11].

Decryption uses the secret key to recover the corresponding plaintext polynomial from the resulting ciphertext. Decoding then transforms this polynomial into a plaintext vector, from which the resulting messages are extracted.

B. Oblivious Message Retrieval

Private signaling (PS) introduced in [7] is a method for transmitting payloads intended for a specific receiver, while concealing the intent of a sender from others. Fig. 1 shows a secure communication process based on PS. Upon receiving a public signal key pk_{sig} from the receiver, the sender generates a signal sig as a clue for the payload x . The sender then posts the sig - x pair on a public bulletin board BB, which accumulates N signal-payload pairs from various senders. The signal is cryptographically constructed so that only the party possessing the secret key (i.e., the intended receiver) can recognize that it is meant for them, while revealing no information otherwise. Although the receiver could download the entire BB

and decrypt all pairs to identify the pertinent payloads, this approach is computationally intensive and imposes significant communication overhead on the receiver.

To address these issues, OMR delegates the scanning task to a resource-rich third-party server known as the detector [1]. OMR employs an HE scheme to detect payloads pertinent to the receiver without exposing any meaningful information to the detector. In existing OMR schemes [1], [6], [7], the receiver typically provides the detector with a detection key pk_{det} , which contains the PS secret keys encrypted under the HE scheme, the public keys for the HE scheme, and an upper bound k indicating the maximum number of pertinent payloads the receiver expects to retrieve.

In SophOMR [7], which is the state-of-the-art OMR scheme, the detector performs two main tasks: homomorphic detection (Detect) and homomorphic compression (Comp). Detect homomorphically computes the indices of pertinent payloads from the bulletin board using the detection key. The results are ciphertexts of a sparse binary vector and serve to mask the pertinent payloads while zeroing out the non-pertinent ones. Although the resulting data is still as large as the original bulletin board, Comp reduces the size. It compresses the encrypted sparse vector into a compact digest D , which is significantly smaller than the bulletin board and ideally proportional to k . Since the signal is cryptographically designed to hide the receiver and the operations involved in Detect and Comp are performed in the HE domain, the detector is unable to determine which payloads are relevant to the receiver. When the digest is sent to the receiver, they decode it using their secret key.

C. Matrix-Vector Multiplication Algorithm in SophOMR

One of the most critical operations in SophOMR is the homomorphic matrix-vector multiplication (MatMul), which multiplies a plaintext matrix \mathbf{M} of size $N \times k$ with a ciphertext \mathbf{v} encrypting a vector of length k , as follows:

$$\mathbf{Mv} = \sum_{i=0}^{k-1} \text{diag}_i(\mathbf{M}) \odot \text{Rot}^i(\mathbf{v}), \quad (1)$$

where $\text{diag}_i(\mathbf{M})[j] = \mathbf{M}[j \bmod N][(i + j) \bmod k]$ and \odot represents multiplication between a plaintext and a ciphertext. To optimize this operation, SophOMR applies the baby-step gaint-step style optimization [12] to MatMul, as follows:

$$\mathbf{Mv} = \sum_{g=0}^{\tilde{g}-1} \text{Rot}^{g\tilde{b}} (\sum_{b=0}^{\tilde{b}-1} \mathbf{m}_{g\tilde{b}+b} \odot \text{Rot}^b(\mathbf{v})), \quad (2)$$

where $k = \tilde{g} \cdot \tilde{b}$ and $\mathbf{m}_{g\tilde{b}+b}$ denotes $\text{Rot}^{-g\tilde{b}}(\text{diag}_{g\tilde{b}+b}(\mathbf{M}))$. This optimization reduces the number of Rot operations from $k = \tilde{g} \cdot \tilde{b}$ to $\tilde{g} + \tilde{b}$, while requiring only two rotation keys. The optimized MatMul algorithm is presented in Algorithm 1.

III. PROPOSED WORK

A. Motivation

This paper focuses on accelerating the detector operations of SophOMR. Specifically, we target the MatMul operation in the Detect phase, which offers high potential for parallelism. The Detect phase is divided into two components: an affine

Algorithm 1 MatMul [7]

Input: $(\mathbf{m}_j)_{j=0}^{k-1}$, \mathbf{ct}_{in}
Output: \mathbf{ct}_{out}

- 1: $\mathbf{ct}_0 \leftarrow \mathbf{ct}_{\text{in}}$
- 2: **for** $(b = 1; b < \tilde{b}; b = b + 1)$ **do**
- 3: $\mathbf{ct}_b \leftarrow \text{Rot}^1(\mathbf{ct}_{b-1})$
- 4: **end for**
- 5: **for** $(g = \tilde{g} - 1; g \geq 0; g = g - 1)$ **do**
- 6: $\mathbf{ct}_{\text{sum}} \leftarrow \sum_{b=0}^{\tilde{b}-1} \text{PCmul}(\mathbf{m}_{g\tilde{b}+b}, \mathbf{ct}_b)$
- 7: **if** $g = \tilde{g} - 1$ **then**
- 8: $\mathbf{ct}_{\text{out}} \leftarrow \mathbf{ct}_{\text{sum}}$
- 9: **else**
- 10: $\mathbf{ct}_{\text{out}} \leftarrow \text{CCadd}(\text{Rot}^{\tilde{b}}(\mathbf{ct}_{\text{out}}), \mathbf{ct}_{\text{sum}})$
- 11: **end if**
- 12: **end for**
- 13: **return** \mathbf{ct}_{out}

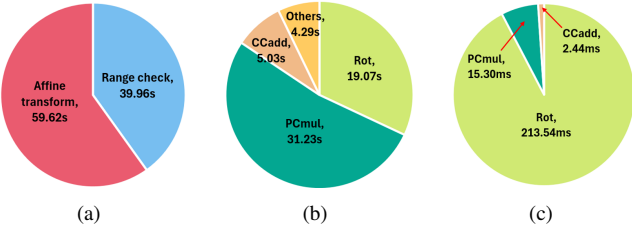


Fig. 2. CPU time breakdown of Detect when $k = 50$ and a single thread is used. (a) Time distribution within Detect for $N = 2^{16}$. (b) Time distribution within MatMul operations. (c) Execution time of individual HE operations.

transform and a range check. While the range check involves more consecutive homomorphic multiplications, a key factor in the performance of HE schemes, the affine transform often exhibits longer execution times. Fig. 2(a) shows the time distribution within the Detect phase with a bulletin board size (N) of 2^{16} , evaluated on a workstation equipped with an Intel Xeon W-2295 processor and 128 GB of RAM. The affine transform takes approximately 1.5 \times longer to execute compared to the range check.

Nearly all the time spent in the affine transform is consumed by MatMul operations. Fig. 2(b) shows a breakdown of the execution time for the MatMul operations. More than 50% of the time is spent on PCmul operations, followed by Rot operations, which account for more than 30%. However, when looking at the execution time of a single operation, Rot takes significantly longer than PCmul, as shown in Fig. 2(c). This implies that accelerating MatMul requires (1) optimizing the Rot operation itself and (2) parallelizing the large number of PCmul operations. To address them, we use multi-level design parameters along with a design space exploration (DSE) technique to find their optimal values.

B. Overall Design Process

Our DSE-based design process is shown in Fig. 3. We first use high-level synthesis (HLS) to get the synthesis results, specifically the latency and hardware resource usage, of each building homomorphic operator used in MatMul. To this end, we extracted the relevant functions from the Microsoft

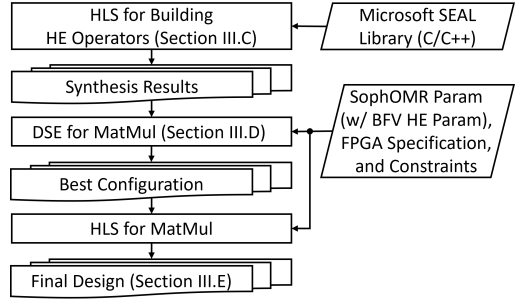


Fig. 3. Overall design process to design our MatMul accelerator.

TABLE I
DESIGN PARAMETERS FOR MATMUL ACCELERATORS

Parallelism type	Related homomorphic operator	Parameter
Coefficient level	CCadd, PCmul, Rot	PC
NTT BU level	Rot	PB
Instance level	PCmul	PI

SEAL open-source library [13] and refactored them for HLS compatibility. Note that although the SophOMR open-source code [14] is based on the OpenFHE library [15], this paper opts for SEAL due to its clearer function hierarchies, which simplify the generation of HLS code. Each homomorphic operator is implemented in multiple versions corresponding to different parameter configurations. The parameter types used in this work are summarized in Table I and described in detail in the following subsections.

Using the synthesis results of the building homomorphic operators together with the cost models presented in Section III-D, DSE is performed for MatMul. Compared to general approaches that rely on coarse-grained modeling and extrapolation to estimate latency and hardware resource usage across design variants, our synthesis-based methodology enables more accurate DSE. During the DSE process, SophOMR parameters, including BFV HE parameters, FPGA specifications, and design constraints are taken into account. Once the optimal feasible design parameters are determined, HLS is reused to generate the final MatMul accelerator.

C. Implementation of Building Homomorphic Operators

For the CCadd and PCmul modules, the HLS PIPELINE pragma with a target initiation interval of 1 is used to maximize throughput. In addition, PC coefficients are processed in parallel to further improve performance. The design parameter PC is also applied to the Rot module, but an additional design parameter is introduced for the KeySwitch module. Within the KeySwitch module, the most time-consuming operations are the NTT and the modular multiplications with rotation keys, which are performed in series. As in [16], our KeySwitch module incorporates limb-based pipelining, allowing the NTT and modular multiplications to be performed in parallel. Since the execution time of the NTT is generally longer than that of the modular multiplication, the overall performance of the KeySwitch module is primarily determined by the NTT latency. The performance of the NTT is directly influenced by the number of butterfly units (BUs) operating

concurrently [17]. Therefore, the number of BUs is defined as a design parameter PB . For NTT implementation, the HLS-based open-source autoNTT library [18] is used, specifically the iterative architecture + Barrett reduction version.

D. Cost Models

Although HLS facilitates the search for optimal design parameters, the design space grows exponentially with the number of tunable parameters. To address this, we define cost models to quickly estimate latency and hardware resource usage in the MatMul accelerator, avoiding the need to run HLS for every design configuration. Note that, following the approach in [16], only digital signal processing (DSP) slices, block RAM (BRAM), and UltraRAM (URAM) are considered for hardware resource cost models, as FPGAs typically have abundant lookup tables (LUTs) and flip-flops (FFs).

1) *Latency*: The latency model incorporates the latency synthesis results for the building homomorphic operators and the design parameters listed in Table I. We begin by defining the latency for each iteration for g in Algorithm 1, without considering any design parameters. The PCmul operations and the CCadd operations for accumulation in line 6 are executed in parallel and pipelined manner. Since the latency of PCmul (L_M) is typically longer than the latency of CCadd (L_A), the latency for line 6 is set to $\tilde{b} \cdot L_M + L_A$. The Rot operation with a rotation amount of \tilde{b} (line 10) is executed in parallel with the PCmul and CCadd operations (when $g \neq \tilde{g} - 1$) since there are no data dependencies between them. Letting the latency of Rot be L_R , the latency for each iteration (IL) is defined as follows:

$$IL = \max\{\tilde{b} \cdot L_M + L_A, L_R\} + L_A. \quad (3)$$

Using (3), the total latency of a single MatMul operation is estimated as follows:

$$TL = (\tilde{b} - 1) \cdot L_R + \tilde{g} \cdot IL. \quad (4)$$

By applying the design parameters to (3) and (4), we obtain (5) and (6), respectively.

$$IL' = \max\{\frac{\tilde{b}}{PI} \cdot L'_M + L'_A, L'_R\} + L'_A, \quad (5)$$

$$TL' = (\tilde{b} - 1) \cdot L'_R + \tilde{g} \cdot IL', \quad (6)$$

where PI denotes the number of PCmul cores operating in parallel, which is detailed in Section III-E. L'_M and L'_A are approximately $\frac{L_M}{PC}$ and $\frac{L_A}{PC}$, respectively. For L'_R , PB is applied to NTT and inverse NTT (INTT), while PC is applied to other sub-modules of KeySwitch. The values of L'_M , L'_A , and L'_R are obtained directly from the synthesis results.

2) *DSP Usage*: Similar to latency, the total usage of DSP slices is estimated based on the synthesis results of the building homomorphic operators. Let d_{op} represent the number of DSP slices used by a homomorphic operator $op \in \{\text{CCadd}, \text{PCmul}, \text{Rot}\}$. Then, the total DSP usage D is calculated as follows:

$$D = (PI + 1) \cdot d_{\text{CCadd}} + PI \cdot d_{\text{PCmul}} + d_{\text{Rot}}. \quad (7)$$

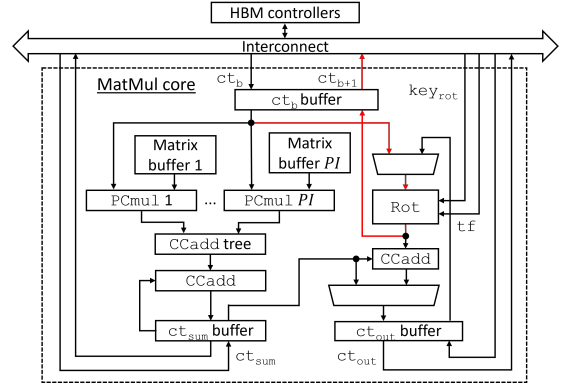


Fig. 4. Simplified MatMul hardware architecture. The red arrows represent the data flow corresponding to lines 2-4 of Algorithm 1.

3) *BRAM and URAM Usage*: In our MatMul accelerator, only the Rot module utilizes BRAMs, specifically within the NTT and INTT modules. URAMs, on the other hand, serve as internal buffers within the Rot module, including rotation key buffers, and are also used for matrix buffers. In addition, URAMs are utilized as data transfer buffers to facilitate communication with off-chip memory. The total URAM usage is obtained by adding all individual values.

E. Hardware Architecture

Fig. 4 shows a simplified block diagram of the proposed MatMul hardware architecture. A single Rot core is instantiated and shared by lines 3 and 10 of Algorithm 1. Within the Rot module, buffers are allocated to store rotation keys. Under the SophOMR parameters (see Table II), a single rotation key occupies 55MB. Since MatMul uses two rotation keys (for shift amounts 1 and \tilde{b}), the total storage of 110MB exceeds the available on-chip memory. Consequently, only a portion of the keys is kept in URAMs and continuously updated with data fetched from off-chip memory. Similarly, the twiddle factors (TFs) used in the (I)NTT are updated from off-chip memory.

The $\tilde{g} \cdot \tilde{b}$ PCmul operations in MatMul are independent of each other. Therefore, the proposed hardware architecture deploys PI PCmul cores running in parallel. Accordingly, $(PI - 1)$ CCadd cores are used to sum the products from the PI PCmul cores, and two additional CCadd cores are used for the accumulation and final ciphertext computation, respectively. Each PCmul core is accompanied by a dedicated matrix buffer. Each m_j in Algorithm 1 is a single plaintext that remains constant. When using the SophOMR parameters (in Table II), its size is approximately 1,280Kb. The MatMul algorithm involves k matrices, which are precomputed and distributed across the PI matrix buffers.

As described in Section III-D, data transfer buffers implemented using URAMs (ct_b , ct_{sum} , and ct_{out} buffers) are deployed to temporarily store ciphertexts during transfers to/from off-chip memory. Due to the large size of a ciphertext, which includes multiple limbs, only a single limb is stored in each data transfer buffer at a time. To hide off-chip memory latency, a double buffering scheme is utilized.

TABLE II
SOPHOMR PARAMETERS

N	t	$[\log Q]$	$[\log PQ]$	$[\log q_i]$	k	\tilde{g}	\tilde{b}
2^{16}	786,433	1,140	1,740	60	50	23	46

TABLE III
TOP FOUR CONFIGURATIONS FROM DSE FOR MATMUL ACCELERATORS

Order	CCadd		PCmul		Rot	
	PC	PC	PC	PI	PC	PB
1 (best)	16	16	2	16	64	
2	16	8	4	16	64	
3	16	4	8	16	64	
4	16	2	16	16	64	

IV. EVALUATION

A. Experimental Setup

The SophOMR parameters are listed in Table II. Here, N represents the total number of payloads posted on the bulletin board, which is equal to the BFV ring dimension n . The plaintext and ciphertext moduli in the BFV scheme are denoted by t and Q , respectively. P is a special modulus used temporarily during the KeySwitch process. The target FPGA platform is an AMD Alveo U55C Accelerator Card, which includes 1,304K LUTs, 2,607K FFs, 2,016 36Kb BRAMs, 960 288Kb URAMs, 9,024 DSP slices, and 16GB HBM2. The AMD Vitis HLS (v2024.1) is used as a development tool.

B. Hardware Implementation Results

Table III shows the top four parameter configurations for the MatMul accelerator, ranked with latency as the highest priority and hardware resource usage as the second, under the constraint of available hardware resources. These configurations show almost identical MatMul latency and resource utilization. Three key insights are drawn from these results. First, since the Rot module is the main performance bottleneck, allocating additional hardware resources to the CCadd and PCmul modules has minimal impact on total latency. Therefore, the Rot module is prioritized in resource allocation. Second, the CCadd module uses significantly fewer hardware resources compared to other modules, allowing its PC value to be large with negligible impact on overall utilization. Finally, remaining resources are allocated to enable PCmul cores to process as many coefficients as possible. Although PC and PI values differ across the four configurations, all are capable of processing 32 coefficients of a ciphertext polynomial in parallel. From a resource perspective, increasing PC is slightly more efficient than increasing PI , as it reduces the number of required CCadd cores. Although not shown in Table III, when PC exceeds 16, the ct_b buffer is enlarged to support the increased bandwidth, reducing the URAM efficiency. In such cases, increasing PI becomes a better option.

Table IV shows the resource utilization, as well as the latency, for each building homomorphic operator and the overall MatMul operator using the best parameter configuration. To the best of the authors' knowledge, this work is the first hardware accelerator for OMR. Therefore, the latency results are compared with those obtained from a CPU-based implementation [14], which are shown in Figs. 2(a) and 2(c).

TABLE IV
FPGA IMPLEMENTATION RESULTS (TARGET FREQ. = 200MHz)

Operator	DSP	BRAM (36Kb)	URAM (288Kb)	Latency (ms) / Improvement
1 CCadd	1	0	0	0.80 / 3.05 \times
1 PCmul	897	0	0	0.80 / 19.13 \times
1 Rot	5,123	1,536	313	31.35 / 6.81 \times
MatMul total	6,920	1,536	659	2,150 / 13.86 \times

Note that in the default setting of [14], the affine transform involves 2 MatMul operations, resulting in MatMul CPU time ≈ 29.8 seconds. Our MatMul accelerator utilizes around 70% of the FPGA resources and achieves a 13.86 \times speedup when scanning 2^{16} payloads, of which up to 50 are pertinent.

V. CONCLUSION

This paper presents an FPGA-based accelerator for the MatMul operation aimed at enhancing the practicality of OMR schemes. We use an HLS technique to boost implementation productivity and improve accuracy in DSE. In addition, we propose cost models to rapidly identify the optimal parameter configuration. The implemented MatMul accelerator achieves a 13.86 \times speedup over the CPU implementation. A limitation is the low performance of the Rot module. Therefore, future work will focus on optimizing this component.

ACKNOWLEDGMENTS

This material is based upon work supported by the National Science Foundation under Grant No. 2347253. The authors thank Dr. Young-kyu Choi for his valuable advice.

REFERENCES

- [1] Z. Liu *et al.*, "Oblivious message retrieval," in *Proc. Crypto*, 2022.
- [2] G. Beck *et al.*, "Fuzzy message detection," in *Proc. CCS*, 2021.
- [3] V. Madathil *et al.*, "Private signaling," in *Proc. USENIX Security*, 2022.
- [4] S. Jakkamsetti *et al.*, "Scalable private signaling," in *Proc. CSF*, 2025.
- [5] J. H. Cheon *et al.*, "Introduction to homomorphic encryption and schemes," *Protecting Privacy through Homomorphic Encryption*, pp. 3–28, 2021.
- [6] Z. Liu *et al.*, "Perfomr: Oblivious message retrieval with reduced communication and computation," in *Proc. USENIX Security*, 2024.
- [7] K. Lee *et al.*, "Sophomr: Improved oblivious message retrieval from simd-aware homomorphic compression," *Cryptology ePrint Archive, Paper 2024/1814*, 2024.
- [8] Z. Brakerski, "Fully homomorphic encryption without modulus switching from classical gapsvp," in *Proc. Crypto*, 2012.
- [9] J. Fan *et al.*, "Somewhat practical fully homomorphic encryption," *Cryptology ePrint Archive, Paper 2012/144*, 2012.
- [10] J.-C. Bajard *et al.*, "A full rns variant of fv like somewhat homomorphic encryption schemes," in *Proc. SAC*, 2016.
- [11] A. S. Özcan *et al.*, "Homomorphic encryption on gpu," *IEEE Access*, vol. 11, pp. 84 168–84 186, 2023.
- [12] S. Halevi *et al.*, "Faster homomorphic linear transformations in helib," in *Proc. Crypto*, 2018.
- [13] "Microsoft SEAL (ver. 3.6)," <https://github.com/Microsoft/SEAL>, 2020.
- [14] "Sophomr," <https://github.com/keewoolee/SophOMR>, 2024.
- [15] A. Al Badawi *et al.*, "Openfhe: Open-source fully homomorphic encryption library," in *Proc. WAHC*, 2022.
- [16] Y. Zhu *et al.*, "Fxhenn: Fpga-based acceleration framework for homomorphic encrypted cnn inference," in *Proc. HPCA*, 2023.
- [17] S. Kim *et al.*, "Hardware architecture of a number theoretic transform for a bootstrappable rns-based homomorphic encryption scheme," in *Proc. FCCM*, 2020.
- [18] D. Kumarathunga *et al.*, "Autontt: Automatic architecture design and exploration for number theoretic transform acceleration on fpgas," in *Proc. FCCM*, 2025.